2007

Epitaxial growth of ZrO2 on GaN templates by oxide molecular beam epitaxy

Xing Gu
Virginia Commonwealth University, gux@vcu.edu

Natalia Izyumskaya
Virginia Commonwealth University

Vitaliy Avrutin
Virginia Commonwealth University, vavrutin@vcu.edu

Bo Xiao
Virginia Commonwealth University, xiaob@vcu.edu

Hadis Morkoç
Virginia Commonwealth University, hmorkoc@vcu.edu

Gu, X., Izyumskaya, N., Avrutin, V., et al. Epitaxial growth of ZrO2 on GaN templates by oxide molecular beam epitaxy. Applied Physics Letters, 91, 022916 (2007).

Epitaxial growth of ZrO_2 on GaN templates by oxide molecular beam epitaxy

Xing Gu,[a] Natalia Izyumskaya, Vitaly Avrutin, Bo Xiao, and Hadis Morkoç
Department of Electrical and Computer Engineering, Virginia Commonwealth University, Richmond, Virginia 23284

(Received 8 March 2007; accepted 10 June 2007; published online 13 July 2007)

Molecular beam epitaxial growth of ZrO_2 has been achieved on GaN (0001)/*c*-Al_2O_3 substrates employing a reactive H_2O_2 oxygen source. A low temperature buffer followed by *in situ* annealing and high temperature growth has been employed to attain monoclinic, (100)-oriented ZrO_2 thin films. The typical full width at half maximum of a 30-nm-thick ZrO_2 (100) film rocking curves is 0.4 arc deg and the root-mean-square surface roughness is ~4 Å. $\omega-2\theta$ and pole figure x-ray diffraction patterns confirm the monoclinic structure of ZrO_2. Data support an in-plane epitaxial relationship of ZrO_2 [010]‖GaN[11$\bar{2}$] and ZrO_2 [001]‖GaN[1$\bar{1}$00]. X-ray diffraction and reflection high-energy electron diffraction analyses reveal in-plane compressive strain, which is mainly due to the lattice mismatch. © *2007 American Institute of Physics*. [DOI: 10.1063/1.2753719]

Zirconium dioxide (ZrO_2) thin films have a wide range of applications such as solid electrolytes,[1] catalysts,[2] and optical coatings.[3] In terms of electronics, ZrO_2 has been considered as a gate dielectric in the realm of scaled down metal-oxide-semiconductor devices,[4] which require the reduction of the thickness of the gate dielectric. For instance, it was pointed out that the equivalent thickness of a gate dielectric should be around 0.8 nm for devices with short gate (~15 nm),[5] which is sufficiently thin for SiO_2 to suffer from direct tunneling current. The above consideration stems from its wide band gap (~5.8 eV), dielectric constant over 20, high breakdown field (15–20 MV/cm), good thermal stability, and large conduction band offset ($\Delta E_c \sim 1.4$ eV) with silicon.[6] The epitaxial growth of ZrO_2 on Si by various methods such as metal organic chemical vapor deposition (MOCVD)[7] and pulsed laser deposition[8] has been reported. Single-crystal oxides grown by molecular beam epitaxy (MBE) can, in principle, avoid grain boundaries while providing a good interface. However, attempts of ZrO_2 epitaxy on Si (100) by MBE using O_2 gas as the oxidant have resulted in polycrystalline ZrO_2.[9,10]

ZrO_2 can also be used as an effective bridge material between complex perovskite oxides and semiconductors, since it helps to accommodate the large discrepancy in crystal structure and lattice constant between the perovskite materials and hexagonal GaN. To make possible the integration of ferroelectric perovskite oxides and semiconductors such as GaN, suitable bridge layers are required to provide a platform for high-quality oxide growth on GaN. In this vein, crystalline, especially single crystalline, ZrO_2 is required. In addition, single crystal ZrO_2 can also be used as a gate dielectric material if sufficiently high quality can be attained. In a somewhat related application, amorphous ZrO_2 has also been explored as a gate dielectric for GaN-based devices by using ultraviolet ozone oxidation of Zr metal[11] or electron beam evaporation.[12] However, epitaxial growth of ZrO_2 on GaN has not been reported to date.

In this letter, we report on the epitaxial growth of ZrO_2 on GaN using oxide MBE. Because of a very low equilibrium pressure of metal Zr, making thermal evaporation exceedingly difficult, zirconium tetra (Zr-t) butoxide was chosen as the metal organic (MO) precursor for Zr. In order to overcome the drawbacks of the conventional oxygen plasma sources such as possible surface damage by high-energy particle and degradation of plasma sources due to the high reactivity of oxygen radicals, a highly reactive H_2O_2 was employed. Already, H_2O_2 has been applied to ZnO(Refs. 13 and 14) and $PbTiO_3$.[15] The crystal structure and surface morphology of the epitaxially grown ZrO_2 thin films were characterized by reflection high-energy electron diffraction (RHEED), x-ray diffraction (XRD), and atomic force microscopy (AFM).

GaN (0001) templates fabricated by on *c*-plane sapphire served as substrates. ZrO_2 thin films reported here were grown in a modified Riber 3200 MBE system using 50% aqueous solution of H_2O_2 as the reactive oxygen source. Zr-t butoxide was kept in a stainless-steel bubbler heated by a water bath, and argon (6*N* purity) was used as the carrier gas. During growth, the temperature of the bubbler for the Zr MO source was kept at 56 °C. The flow rate of the Ar carrier gas was controlled by a mass flow controller and the flow rate values used in this work ranged between 1 and 2 SCCM (SSCM denotes cubic centimeter per minute at STP), which resulted in growth rates in the range of 10–20 nm/h. The ZrO_2 films were grown under oxygen-rich conditions and the pressure of H_2O_2 used was kept from 1.5 to 3.0×10^{-5} Torr. The growth evolution of ZrO_2 by MBE was monitored *in situ* by a RHEED system. Figure 1 displays a RHEED pattern of the GaN template before the growth was initiated and a set of ZrO_2 patterns taken at different stages of ZrO_2 growth. The diffraction pattern of ZrO_2 (011) is rotated about 15° from both the GaN (11$\bar{2}$0) and GaN (1$\bar{1}$00) directions. At the initial stages of the growth, a few monolayers of ZrO_2 were deposited on the GaN template at a low temperature (LT) of 300 °C to minimize the potential oxidation of GaN which has a strong tendency to occur at higher temperatures. Without such a LT buffer layer, the RHEED pattern of ZrO_2 grown at 700 °C showed a highly *a*-textured (100) structure

[a]Electronic mail: gux@vcu.edu

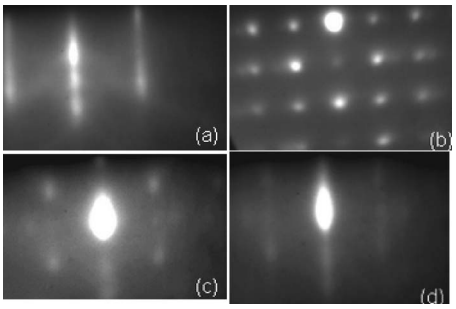

FIG. 1. RHEED pattern of (a) GaN $(11\bar{2}0)$ and (b) of ZrO_2 (011) grown high temperature without buffer layer (c) during growth of low temperature ZrO_2 (011) buffer layer, and (d) during high temperature growth ZrO_2 (011).

[see Fig. 1(b); the pattern did not change when the sample was rotated], which can be caused by the above-mentioned oxidation of GaN at high temperatures. The LT-ZrO_2 exhibits a three-dimensional (3D) RHEED pattern, as shown in Fig. 1(c). To combat this issue, the LT ZrO_2 thin buffer was then annealed *in situ* at 750 °C with H_2O_2 flow. A noticeable surface flattening was observed at annealing temperatures above 700 °C, as indicated by the transition from a 3D spotty RHEED pattern to a two-dimensional (2D) streaky one [Fig. 1(d)]. The high temperature (HT) growth of ZrO_2 with a total thickness of 30 nm was then performed at 700 °C, and the streaky RHEED pattern remained.

The surface morphology of the epitaxially grown, 10-nm-thick ZrO_2 was examined by AFM (see Fig. 2). The AFM image indicates a smooth and uniform oxide thin film with a rms value of ~4 Å for the 5×5 μm^2 image. The ZrO_2 layer is contiguous, and some features of the atomic steps from the MOCVD GaN template remain observable. The continuous feature of the film is a hallmark of good epitaxy, and is imperative for ZrO_2, to be used as "bridge layers" for the potential ferroelectric/semiconductor integration and gate dielectric.

Figure 3(a) shows the XRD ω-2θ pattern of a 30-nm-thick ZrO_2 grown on GaN (0001)/c-Al_2O_3. XRD high resolution scan was used in this characterization and Ge [200] four-crystal monochromator was used in the incident beam. No mask was used in the rocking curve scan so that the diffraction beam optics acceptance angle is reasonably large. The peak position of ZrO_2 reflection is consistent with (100) reflection of monoclinic ZrO_2. In other words, the out-of-plane epitaxial relationship for the growth of ZrO_2 on GaN (0001) is ZrO2 (100)‖GaN (0001). The out-of-plane lattice constant $a=5.203$ Å of ZrO_2 was deduced from the

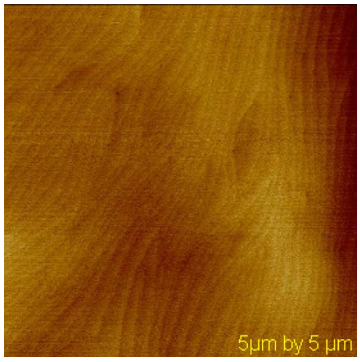

FIG. 2. (Color online) AFM image of a 10-nm-thick ZrO_2 on GaN. The image size is 5×5 μm^2 and rms is 4 Å.

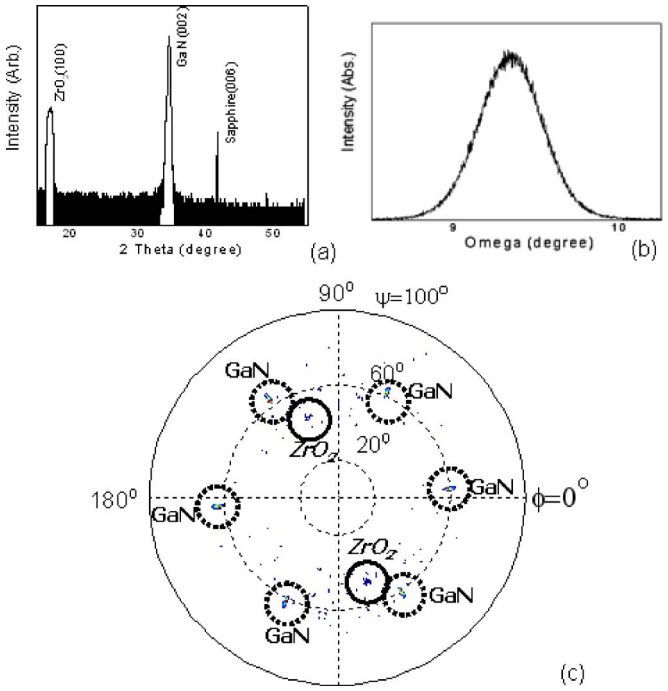

FIG. 3. (Color online) (a) ω-2θ XRD pattern of ZrO_2/GaN. (b) Rocking curve of ZrO_2(100). (c) XRD pole figure scan of ZrO_2 (101) and GaN (10−11).

peak position using the sapphire (0006) reflection as reference. A comparison with the bulk value of $a_0=5.169$ Å indicates that the ZrO_2 thin film is under in-plane compressive strain and the layer is not fully relaxed yet. (The out-of-plane misfit strains were determined by using $\varepsilon\| = (a-a_0)/a$, where $a=5.203$ Å is the value calculated from the diffraction position in XRD high resolution scan, and $a_0=5.169$ Å is the bulk value.) The rocking curve of the ZrO_2 (100) reflection is plotted in Fig. 3(b) and the full width at half maximum (FWHM) of the peak is 0.4 arc deg. This value is considerably small for such a thin film and is indicative of the decent crystalline quality of the epitaxially grown ZrO_2.

The residual (or biaxial compressive/tensile) strain in ZrO_2 layers on GaN templates can have its genesis in either lattice or thermal mismatch between these two materials. In order to clarify the dominant source of the strain, we have compared the strain calculated from XRD patterns, which reflects the strain condition in the layer after it was cooled down, with that at the growth temperature (700 °C). The latter value can be extracted from RHEED patterns utilizing the separation between the reflections which is inversely dependent of the lattice constant. It should be noted that, at the growth temperature, epitaxial ZrO_2 does not suffer from strain caused by the thermal expansion mismatch and, therefore, the strain calculated from the RHEED pattern recorded at this temperature is a pure representation of the lattice mismatch. The thermal expansion coefficient α for monoclinic ZrO_2 along the b and c directions (monoclinic ZrO_2 has $b=5.24$ Å and $c=5.37$ Å while $\beta=99.1°$) is 1.35×10^{-6} and 14.68×10^{-6} K^{-1}, respectively, while that for wurtzitic GaN along the a direction is 5.59×10^{-6} K^{-1}. Therefore, the lattice constant a of GaN at 700 °C can be estimated using $a=a_0(1+\alpha_a\Delta T)=3.203$ Å, where $a_0=3.191$ Å deduced from the XRD pattern measured at room temperature. Since $\alpha=90°$ in monoclinic ZrO_2, $d_{(011)}$, the interplane distance of ZrO_2 (011) can be estimated as $d=bc/\sqrt{b^2+c^2}$, while the

distance between the GaN $(11\bar{2}0)$ reflection plane is $\sqrt{3}a/2$. Therefore, we can calculate the in-plane distance for ZrO_2 (011) as 3.71 Å. On the other hand, the d value for the bulk ZrO_2 at 700 °C was calculated as 3.83 Å, which confirms the in-plane compressive strain when compared with the value of 3.71 Å found from the RHEED patterns. This result is in good agreement with the XRD data which also reveal in-plane compressive strain in the ZrO_2 film at room temperature. Moreover, the difference in the distance between the RHEED reflections of ZrO_2 at 700 and 100 °C was below the resolution of our measurements, which suggests that the strain in ZrO_2 grown by MBE is primarily due to lattice mismatch.

It is well known that the ZrO_2 has three different crystalline structures: the monoclinic structure (baddeleyite) is stable at low temperatures; as temperature rises to around 1400 K, ZrO_2 undergoes a first order martensitic phase transition into the tetragonal structure; and a further increase in temperature to 2570 K renders the ZrO_2 to assume the cubic structure (fluorite) which is stable at very high temperatures. Compared to monoclinic ZrO_2, which typically has a dielectric constant around 20–24, the tetragonal ZrO_2 possesses a dielectric constant of up to 35–50 (Ref. 16), despite the fact that polarization at the atomic level is reduced. Dopants such as yttria can stabilize high-temperature forms of zirconium dioxide partially or fully at room temperature, making the yttria-stabilized zirconia (YSZ) tetragonal or cubic (when fully stabilized) and thus raising dielectric constant effectively. In this work, however, monoclinic ZrO_2 was achieved.

An x-ray pole figure analysis was performed in order to confirm the monoclinic structure of the ZrO_2 and determine the epitaxial relationships. The x-ray pole figure recorded with 0.5° scan steps for φ and 1° steps for ψ angles (the scan ranges were 0 to 360° and 0 to 90° for φ and ψ, respectively) is shown in Fig. 3(c). The peaks with the sixfold symmetry correspond to the GaN $(10\bar{1}1)$ reflections. Compared with the reflections of GaN, the peaks corresponding to ZrO_2 are relatively weak and broad, in part due to the small thickness of the film. However, it is still possible to confirm that the reflection of ZrO_2 (101) is of twofold symmetry, consistent with the monoclinic structure, while it should be four-fold symmetric for tetragonal ZrO_2.

The ω-2θ XRD patterns discussed above indicate that the out-of-plane epitaxial relationship is ZrO_2 (100)∥GaN (0001). From our observations of RHEED, the symmetric pattern corresponding to ZrO_2 [011] azimuth always appeared around 15° rotated with regards to GaN $[11\bar{2}0]$ From the pole figures, the angle between the GaN and ZrO_2 reflections is also close to 15°. Based on these findings, we can propose the in-plane epitaxial relationship for ZrO_2/GaN heterostructures. In this vein, Fig. 4 illustrates the possible in-plane alignment of ZrO_2 and GaN lattices. The reflection plane (011) of ZrO_2 has 14.3° and 15.7° rotations from GaN$(11\bar{2}2)$ and GaN$(1\bar{1}00)$, respectively $[\arctan(c/b) = 45.7°$; see Fig. 4], and an in-plane epitaxial relationship of $ZrO_2[010]$∥GaN$[11\bar{2}0]$ and $ZrO_2[001]$∥GaN$[1\bar{1}00]$ is suggested.

In summary, epitaxial ZrO_2 has been grown on GaN $(0001)/c$-Al_2O_3 by oxide MBE using H_2O_2 as reactive oxygen source and Zr-t butoxide as Zr precursor. To achieve 2D growth mode, a two-step process was adopted: LT deposition of thin buffer layer at 300 °C followed by *in situ* annealing at 750 °C and HT growth at 700 °C. AFM studies revealed a smooth surface with rms value for 5×5 μm^2 scans of about 4 Å. The FWHM of the ZrO_2 (100) rocking curve is 0.4 arc deg for a 30 nm layer. The structural studies indicate that monoclinic (100)-oriented ZrO_2 results in GaN (0001). At room temperature, the films are under in-plane compressive strain. Comparison of lattice parameters determined from RHEED patterns at the growth temperature with those calculated by taking into account the thermal expansion points out that this strain is most likely due to the lattice mismatch. The lattice parameters calculated from the RHEED patterns indicate that the in-plane compressive strain in the ZrO_2 films is present already at the growth temperature. This again supports the suggestion that the strain is most likely due to the lattice mismatch. Based on the RHEED and XRD patterns, the in-plane epitaxial relationship is found to be $ZrO_2[010]$∥GaN$[11\bar{2}0]$ and $ZrO_2[001]$∥GaN$[1\bar{1}00]$.

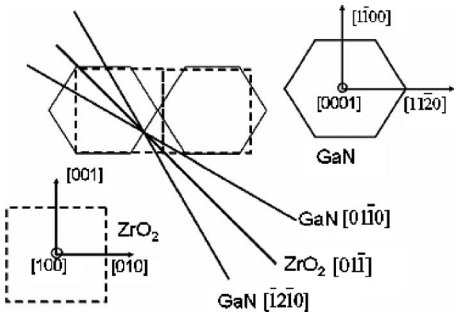

FIG. 4. Proposed in-plane epitaxial relationship between ZrO_2 and GaN.

This work is supported by a grant from the Office of Naval Research under the direction of C. E. C. Wood.

[1] S. P. S. Badwal, F. T. Ciacchi, and D. Milosevic, Solid State Ionics **136**, 91 (2000).
[2] A. Corma, Chem. Rev. (Washington, D.C.) **95**, 559 (1995).
[3] N. K. Sahoo and A. P. Shapiro, Appl. Opt. **37**, 8043 (1998).
[4] R. E. Nieh, C. S. Kang, H.-J. Cho, K. Onishi, R. Choi, S. Krishnan, J. H. Han, Y.-H. Kim, M. S. Akbar, and J. C. Lee, IEEE Trans. Electron Devices **50**, 333 (2003).
[5] *The National Technology Roadmap for Semiconductors Technology Needs* (Semiconductor Industry Associations, San Jose, CA, 2004), Vol. I, p. 9.
[6] B. Kralik, E. K. Chang, and S. G. Louie, Phys. Rev. B **57**, 7027 (1998).
[7] A. Sandell, P. G. Karlsson, J. H. Richter, J. Blomquist, P. Uvdal, and T. M. Grehk, Appl. Phys. Lett. **88**, 132905 (2006).
[8] S. J. Wang, Y. F. Dong, C. H. A. Huan, Y. P. Feng, and C. K. Ong, Mater. Sci. Eng., B **118**, 122 (2005).
[9] Jang-Hyuk Hong, Woo-Jong Choi, Doo-Soo Kim, and Jae-Min Myoung, J. Vac. Sci. Technol. B **21**, 2105 (2003).
[10] Myoung-Seok Kim, Young-Don Ko, Jang-Hyuk Hong, Min-Chang Jeong, Jae-Min Myoung, and Ilgu Yun, Appl. Surf. Sci. **227**, 387 (2004).
[11] Y. Dora, S. Han, D. Klenov, P. J. Hansen, K. S. No, U. K. Mishra, S. Stemmer, and J. S. Speck, J. Vac. Sci. Technol. B **24**, 575 (2006).
[12] K. Balachander, S. Arulkumaran, H. Ishikawa, K. Baskar, and T. Egawa, Phys. Status Solidi A **202**, R16 (2005).
[13] N. Izyumskaya, V. Avrutin, W. Schoch, A. El-Shaer, F. ReuB, Th. Gruber, and A. Waag, J. Cryst. Growth **269**, 356 (2004).
[14] A. El-Shaer, A. Bakin, A. C. Mofor, J. Bläsing, A. Krost, J. Stoimenos, B. Pécz, M. Kreye, M. Heuken, and A. Waag, Phys. Status Solidi B **243**, 768 (2006).
[15] X. Gu, N. Izyumskaya, V. Avrutin, H. Morkoç, T. D. Kang, and H. Lee, Appl. Phys. Lett. **89**, 122912 (2006).
[16] X. Zhao and D. Vanderbilt, Phys. Rev. B **65**, 075105 (2001).